First observations in degradation testing of planar magnetics

Shen, Zhan; Wang, Qian; Shen, Yanfeng; Wang, Huai

Published in:
Proceedings of 2019 IEEE Annual Applied Power Electronics Conference and Exposition (APEC 2019)

DOI (link to publication from Publisher):
10.1109/APEC.2019.8721770

Publication date:
2019

First Observations in Degradation Testing of Planar Magnetics

Zhan Shen*, Qian Wang†, Yanfeng Shen*, and Huai Wang*

*Center of Reliable Power Electronics (CORPE), Department of Energy Technology
Aalborg University, Aalborg, Denmark
† Department of Energy Technology, Aalborg University, Aalborg, Denmark
zhs@et.aau.dk, qiw@et.aau.dk, yaf@et.aau.dk, and hwa@et.aau.dk

***Abstract*— Magnetic components are usually assumed relatively reliable in power electronic converters. Nevertheless, with the trend for ever-increasing power density, planar magnetics may need to be designed with reduced margins in terms of thermal and insulation. Wear out or even failure of magnetic components may become an issue in extreme design and operation scenarios. This paper presents the first observations in degradation testing of planar magnetics at high temperatures. It serves to investigate the change of various parameters and identify possible ones as the health indicators of magnetic components for power electronic applications. The degradation testing and characterization results are presented and interpreted.**

***Keywords*—Planar transformer, loss, impedance, degradation, reliability.**

I. Introduction

Planar transformers are preferred in high-frequency and high-power-density power electronics, for their low profile, large heat dispassion surface and easy mass production capability with small parameters variation[1, 2]. Nevertheless, planar transformers become more and more stressed in perspective of reliability due to the following reasons:

- more harmonic electro-magnetic excitations lead to severe high frequency effects, e.g., skin and proximity effects, which increase component losses and temperature;
- commercial power electronic products require a design solution with a competitive cost, which means a small design margin and deteriorated reliability performance;
- the increase of voltage and power density requires a more reliable insulation which can deal with high voltage and high temperature;
- emerging applications (e.g., precision drive, medical, aerospace, more electrical aircrafts, etc.) require high indexes in aspects of volume and reliability.

The reliability challenges are classified as external and internal stresses, as illustrated in Fig. 1. Normally, planar transformers are constructed with planar cores and printed circuit boards (PCB) windings, while insulation layers or tapes are inserted in between to provide isolation function. The failure of magnetics means the lose of power transfer function due to the insulation breakdown, core failure, winding short circuit, thermal runaway, and degradation, etc. The degradation refers to the shift of electromagnetic parameters, e.g., parasitic capacitance, inductance, resistance and core losses, etc. The physics-of-failure (PoF) approach through long-time reliability tests is essential to understand the failure mechanisms of planar magnetics in power electronics [3].

From a component level of view, the failure of planar magnetics mainly comes from the magnetic cores, insulation, and printed circuit boards (PCBs). The degradation of the magnetic core is attributed to the localized overheating, distorted magnetic flux, internal and external magnetic force, and even the shape and volume of the core [4]. They may cause the crystallization, oxidation and other reactions of the core [5]. The degradation can be identified by the characteristic parameters, such as the loss density and permeability. They are regarded as particular for iron power core materials which usually contain organic content [4, 5]. However, recent research reports the Cobalt-doped Mn–Zn ferrite also subjects to aging under thermal stress [6]. The core loss permanently increases at 100 kHz while decreases above 500 kHz. On the other side, the core loss shows a reversible increase under a magnetic field and no changes under humid environment. The mechanism of thermal aging for MgMnFeO ferrites was analyzed early in 1967 [7]. The decline of ferrite permeability is also realized in telecommunications applications [8], and is expressed as the disaccommodation factor D_f. The amorphous alloy cores for low and medium frequency applications are tested in [9]. Both the increase of core loss and x-ray diffractograms indicate the aging after two years. There is mature research on the insulation in power transformers. The degradation of insulation is identified by the degree of polymerization (DP), which is the average length of the cellulose rings or molecule structure in oil and dry type insulation paper, respectively [10]. Based on the failure mechanism related to the DP value, the Arrhenius equation is adopted in the power transformer loading guide for lifetime calculation [11]. This equation is also used for the insulation lifetime prediction in electrical machines and wires under thermal stress [12, 13]. Compared with the normal insulation wire, PCB windings have complex structures, and therefore are relatively vulnerable to vibration and thermal stresses. In [14], the failure mechanism of the PCBs by the flux residue, electric field, temperature, and humidity is investigated; however no lifetime model has been developed.

From a system level point of view, the American military handbook established a classic reliability model for transformers in 1991 [15]. However, most of the coefficients have been

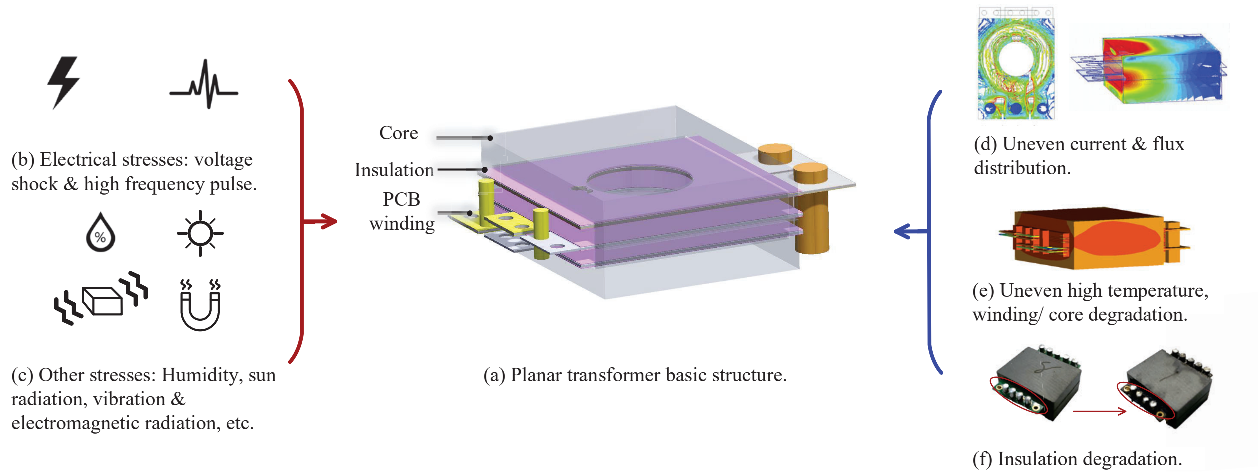

(a) Planar transformer basic structure.

(b) Electrical stresses: voltage shock & high frequency pulse.

(c) Other stresses: Humidity, sun radiation, vibration & electromagnetic radiation, etc.

(d) Uneven current & flux distribution.

(e) Uneven high temperature, winding/ core degradation.

(f) Insulation degradation.

Fig. 1: Basic structure of a planar transformer (a) and its external reliability stresses (b, c) and internal reliability stresses (d, e, f).

outdated nowadays, and the method to gain these values is unknown. The lifetime model in [16] has the similar formula form with that in [15], and it is used by manufacturers for the lifetime calculation of planar transformers [17]. There are more degradation tests for different kinds of magnetics, e.g. power transformer, electrical machine, insulation winding, in [12, 13]. However, planar magnetics have unique and more compact structures, and may suffer from different reliability stresses, as aforementioned. Therefore, systematic test and research on the degradation of planar magnetic components need to be covered.

This paper presents the first observations in the degradation tests of planar magnetics. Test set-ups are built to evaluate various parameters through aging period. Two thermal stresses are exerted to three kinds of core materials and two kinds of planar transformers. Moreover, the failure mechanism and the health indicators of planar magnetics are investigated, which can be further used for the lifetime modeling and prediction.

II. Test Setup and Specimen

A. Core Test Setup

A widely-used two-winding method [18] is adopted for characterizing the power loss measurement of core materials, as illustrated in Fig. 2. Two windings with the same specifications are wiring around the core. They are with the same number of turns and perform as the primary and secondary windings of a transformer. The primary winding is connected to the power amplifier, while the secondary winding is open-circuited. The excitation current through the primary winding and the induced voltage across the secondary winding are measured by the Newtons4th Precision Power Analyzer PPA5500. The total loss generated by the transformer is obtained as the core loss. The secondary winding is open-circuited, thus the transfer current i_t is neglectable, $I_1 \approx I_\mathrm{m}$ and $V_2 \approx V_\mathrm{m}$. The measured loss is regarded as the core loss by R_m. Both windings are with only five turns and Litz wires are used, so the winding loss is negligible.

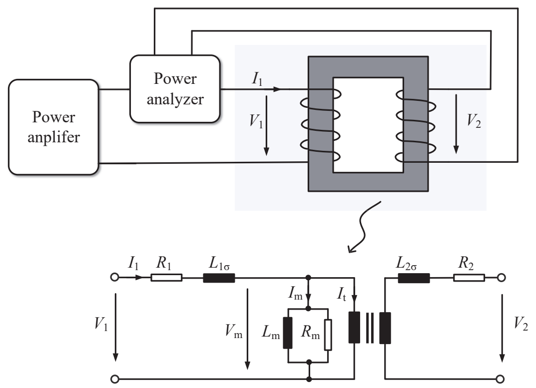

(a) Core loss measurement method and the equivalent circuit of a transformer.

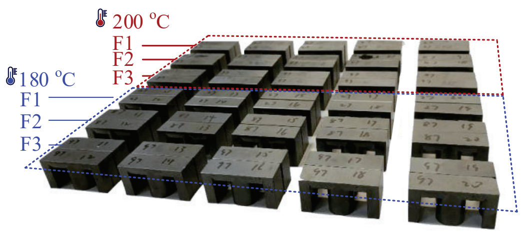

(b) Three kinds of core materials (F1, F2 and F3) and the applied thermal stresses (180 °C and 200 °C).

Fig. 2: Core loss test method and three kinds of core materials under test.

The permeability of the material is measured with the Keysight impedance analyzer E4990A. The secondary winding is connected to the analyzer for the inductance value L_i. The permeability of the material μ_i is then calculated as:

$$\mu = \frac{L_\mathrm{i} l}{N^2 \mu_0 A}, \tag{1}$$

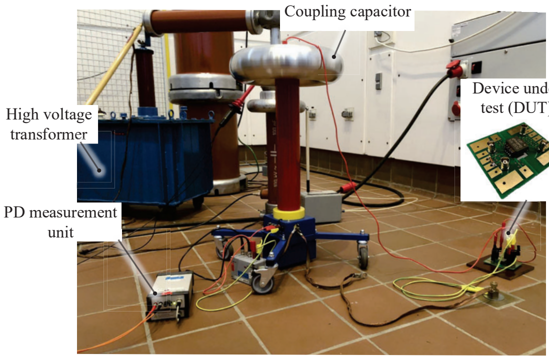

(a) The experimental set up in high voltage lab.

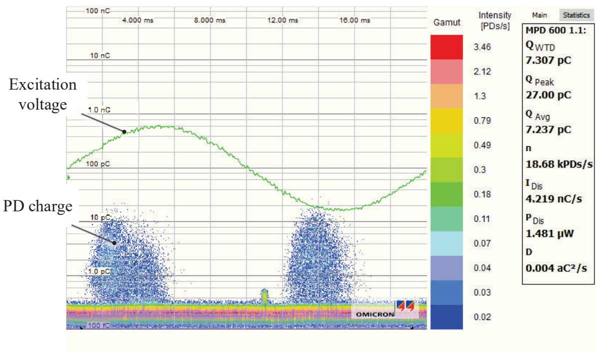

(b) A typical partial discharge test results.

Fig. 3: Transformer insulation test setup and a typical partial discharge waveform.

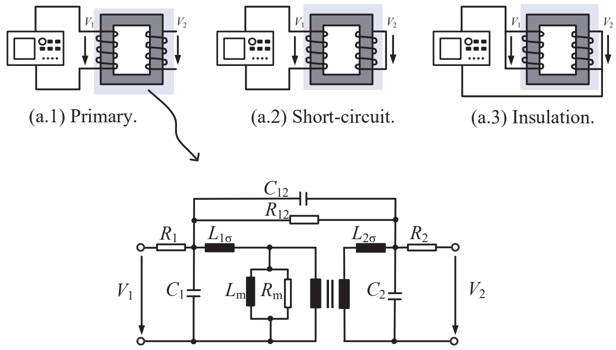

(a.1) Primary. (a.2) Short-circuit. (a.3) Insulation.

(a.4) General equivalent circuit of the planar transformer.

(a) The measurement configurations and equivalent circuit.

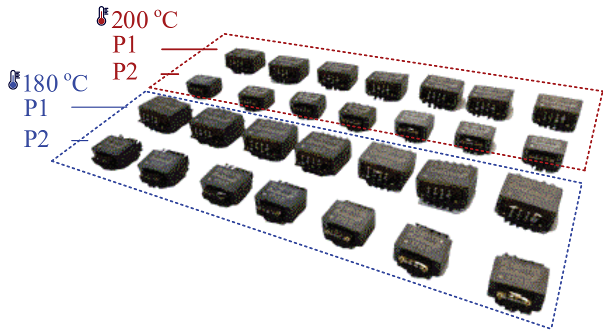

(b) Two types of planar transformer specimens with two thermal stresses.

Fig. 4: Planar transformer measurement configurations and specimens. Configuration (a.1) is to obtain L_{m} + $L_{1\sigma}$ and R_{m}+ R_1, configuration (a.2) is to obtain $L_{1\sigma}$ + $L_{2\sigma}$ and R_1+ R_2, and configuration (a.3) is to obtain C_{12} and R_{12}, respectively.

where l is the average path length of a core, N is the number of turns of a winding, μ_0 is the permeability of vacuum.

For the state of standardization and convenience, all the tests are done with EE cores instead of toroids or planar cores. Only one bobbin set wiring both primary and secondary is used for all tests to ensure the same winding configurations. The surface of each EE core pair is not perfectly smooth, and there may be small air-gaps in between. So the two cores are always pressed tightly to reduce this influence. Moreover, the unsooth surface is inherent for each core and will not affect the parameter change trend on which this paper focuses. Three kinds of ferrites with the same core shape are used, marked as F1, F2 and F3. Each group consists of 5 sets, which are ferrite also commonly used for planar cores. They are placed in 180 °C and 200 °C ovens, and each temperature is with five sets, as is illustrated in Fig. 2(b).

B. Insulation Test Setup

To provide the functionality of transformers, the insulation is one of the key components which affect the reliability of the transformer. The partial discharge (PD) is a localized electrical discharge, which only partially bridges the insulation between conductors [19]. PD measuring is widely used for power transformer to detect the degradation and aging of insulation.

The test is performed under IEC STANDARD 60270 [20]. The test set-up for the planar transformer and a typical phase resolved PD pattern is illustrated in Fig. 3. Due to the frequency limitation of the voltage source and high voltage transformer in the high voltage lab, the test is done at 50 Hz. The discharge is expected to be different in the kHz range, in which the planar transformer operates. However, the 50 Hz results can still indicate the insulation characterization. Two types of planar transformers, grouped as P1 and P2, are tested and shown in Fig. 4(b). Each type is with 16 samples, numbered 1 to 16. No. 1 to No. 7 are for 200 °C thermal stress, while No. 9 to No. 15 are 180 °C, respectively. No. 8 and No. 16 are kept in the room temperature for comparison. Transformers are soldered on the text boards, it is shown in Fig. 3(a) as the device under test (DUT).

C. Transformer Test Setup

System-level planar transformer tests have also been conducted with the samples in Fig. 4(b). The test board in Fig. 3(a) is also used here. Three kinds of test connections are performed for each transformer, as given in Fig. 4(a). The tests are carried out with the Keysight impedance analyzer E4990A, and the excitation voltage is a constant value of 0.5 V.

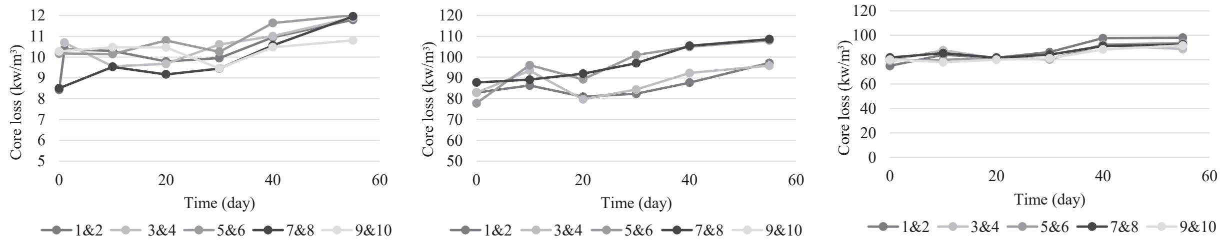

(a) Losses of material F1, 54.5 mT (b) Losses of material F2, 133 mT (c) Losses of material F3, 133 mT

(d) Permeability of material F1 (e) Permeability of material F2 (f) Permeability of material F3

Fig. 5: Core losses and induced flux results during 55 days of 200 °C thermal stress, tested at 20 kHz, one set of F 2 core is broken during the test in 40 days.

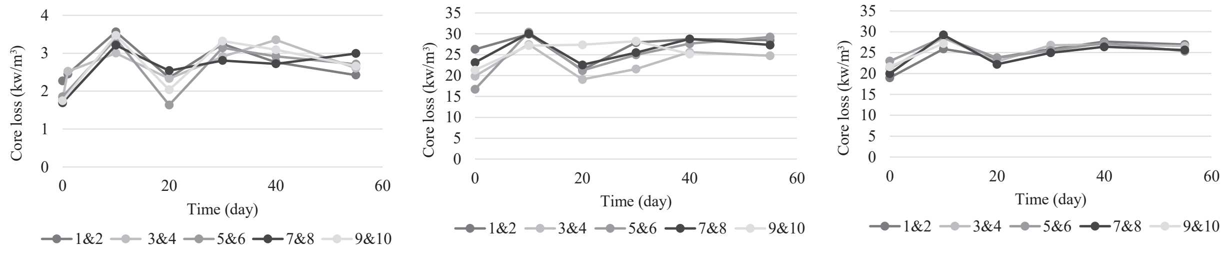

(a) Losses of material F1, 11.8 mT (b) Losses of material F2, 26.2 mT (c) Losses of material F3, 26.2 mT

(d) Permeability of material F1 (e) Permeability of material F2 (f) Permeability of material F3

Fig. 6: Core losses and induced flux results during 55 days of 200 °C thermal stress, tested at 200 kHz, one set of F 2 core is broken during the test in 40 days.

The impedance of the test board is measured before and then subtracted from the measurement results of specimens.

To eliminate the impact of the test board, the test board is tested first with the impedance and phase of Z_{board} and θ_{board}, respectively. With the testing results of the ith planar transformer on the test board Z_{it} and θ_{it}, the impedance of the ith transformer itself is obtained by:

$$\begin{aligned} Z_{ix} &= Z_{it}\cos(\theta_{it}) - Z_{\text{board}}\cos(\theta_{\text{board}}), \\ Z_{iy} &= Z_{it}\sin(\theta_{it}) - Z_{\text{board}}\sin(\theta_{\text{board}}), \end{aligned} \tag{2}$$

$$Z_i = \sqrt{Z_{ix}^2 + Z_{iy}^2}, \quad \theta_i = \arctan\frac{Z_{ix}}{Z_{iy}}. \tag{3}$$

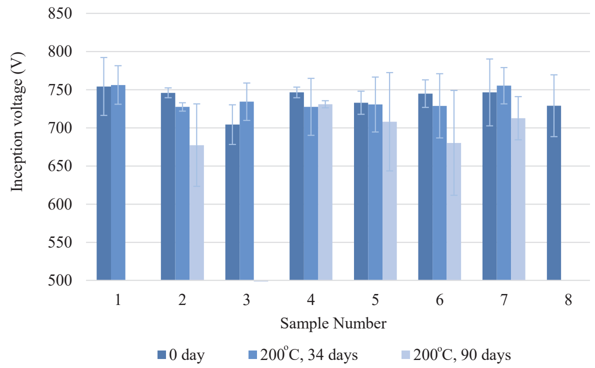

(a) Partial discharge results of inception voltage, P1, 200 °C.

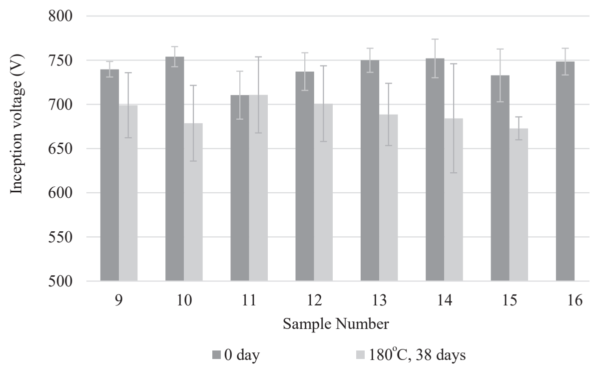

(b) Partial discharge results of inception voltage, P1, 180 °C.

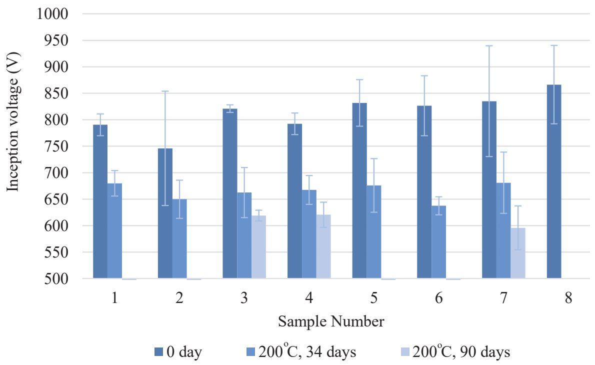

(c) Partial discharge results of inception voltage, P2, 200 °C.

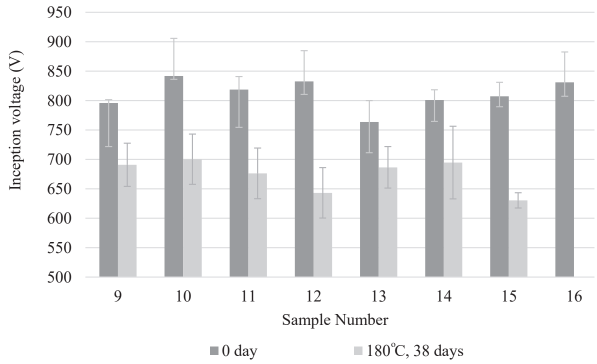

(d) Partial discharge results of inception voltage, P2, 180 °C.

Fig. 7: Insulation test of planar transformer P1 and P2 with thermal stresses in 180 °C and 200 °C. Three times of tests are performed for each point, the inception voltage are the average value and the standard deviation is also given as the error bar. Several transformers are failed or with unreasonable results, and no inception voltage is given.

III. Accelerated Lifetime Tests with Thermal Stress

A. Core Test

The core loss and permeability of cores are tested for the 55 days of thermal stress at 200 °C. Two frequency points (20 k and 200 kHz) are selected for the test and the results are given in Fig. 5 and Fig. 6, respectively. The test is performed each time after the core is taken out of the oven and naturally cooled down till room temperature. At 20 kHz, the excitation voltages of the amplifier are 5.9, 14.5 and 14.5V for material F1, F2, and F3, and the induced flux density B in the core are 54.5, 133 and 133 mT. At 200 kHz, the excitation voltage are 12.8, 28.5, 28.5V and the flux density are 11.8, 26.2, 26.2 mT, respectively. Due to the limited page space and slow degradation process, the testing points of 180 °C are not given. The results will be reported in a following paper.

It can be seen that there is a continuous loss increase with the increase of time in both frequency. In the low frequency range, the hysteresis loss dominates, while at higher frequencies, the eddy current loss is the dominant loss. The test results indicate a large loss absolute value increment of the materials in high frequencies, while similar loss percentage increases in both frequencies. It shows that the ferrite not only has different initial loss in different frequencies, but also with different loss density increment with thermal aging at different frequencies.

The permeability at two frequencies, however, shows almost same value and change trend with the aging process. The test results vary and are difficult to conclude a change trend for the permeability. This is probably due to the slow change ratio of permeability, and the test with two EE cores is largely affected by the air gap although they are pressed tightly in each test. The thermal stress is still applying on the cores, and toroidal cores will be tested in the next step. More results and will be reported in a future paper.

Finally, the cores are becoming more and more smelly, and the color of the core is changing from *black* to *grey*, which is also an indication of the degradation.

B. Insulation Test

With the increase of the applied voltage, partial discharge (PD) starts to occur in the insulation. When the measured PD level exceeds 10 pC, it is regarded as a PD inception in the insulation. PD inception voltage, which the voltage at which PD is triggered, are measured. The measured PD inception voltages for different samples are shown in Fig. 7. Several transformer is failed, as is summarized in Table I.

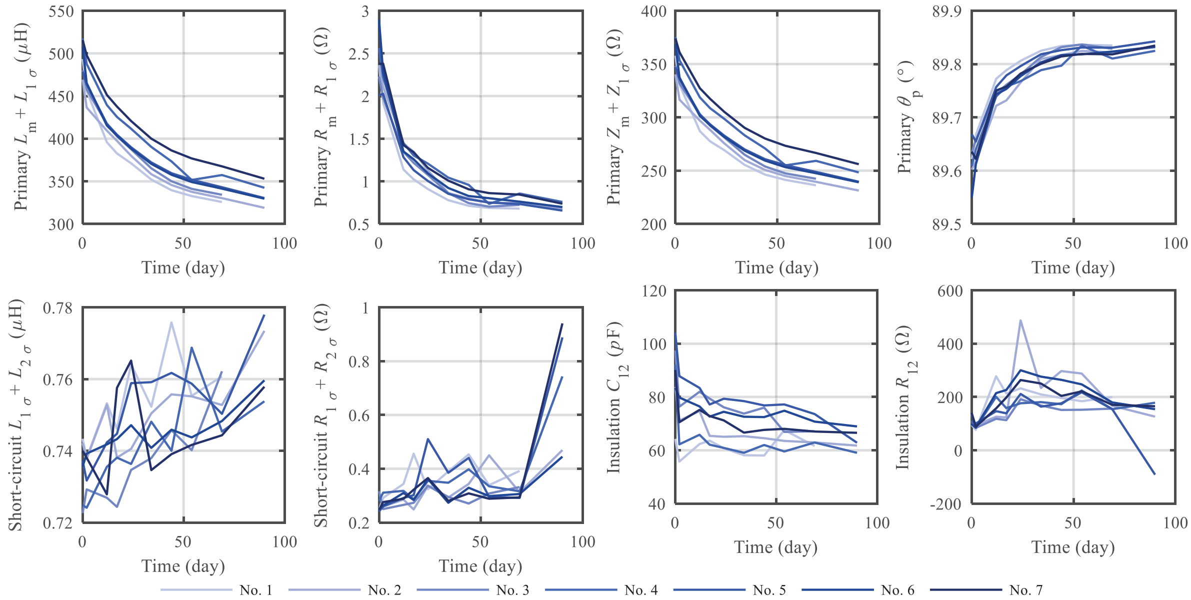

Fig. 8: Test results of No. 1 to 7 planar transformers in P1 group, 200 °C, 90 days, the related parameters are illustrated in Fig. 4(a).

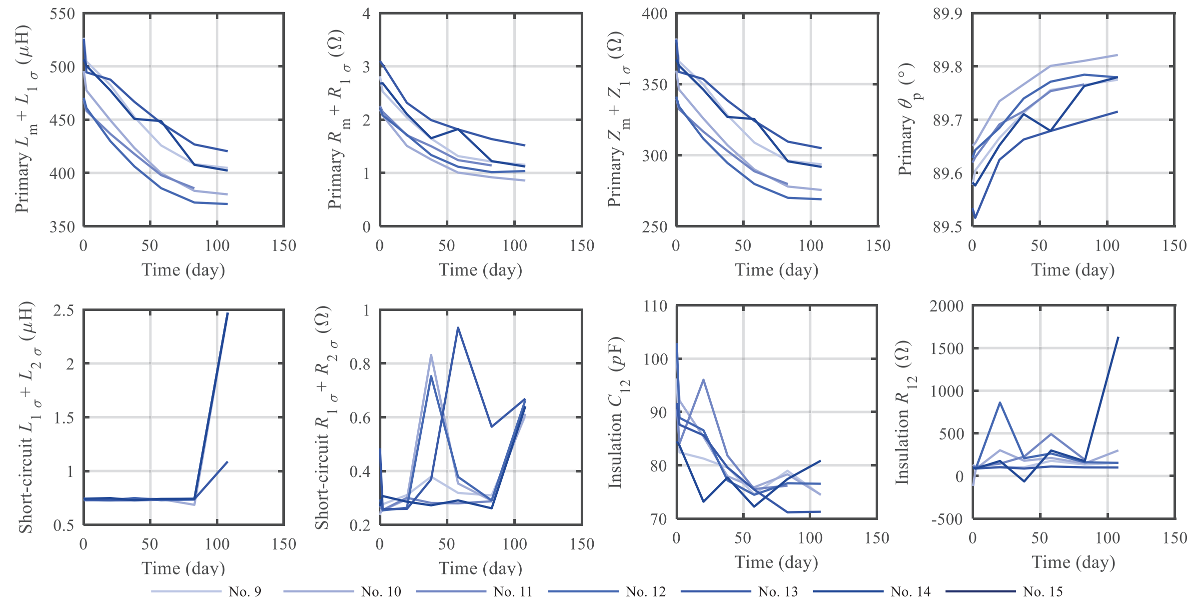

Fig. 9: Test results of No. 8 to 15 planar transformers in P1 group, 180 °C, 108 days, the related parameters are illustrated in Fig. 4(a).

Compared with the initial values (0 day), the inception voltage decreases with the thermal aging process. Normally, it means the degradation of the insulation, and the partial discharge happens more easily. Thus the thermal stress has an impact on the degradation of the insulation system. The inception voltage of P1 after 34 days (200 °C) is almost the same as the 0 day result. It is reasonable to have the hypothesis that the non-change is due to the difference in its insulation system.

C. Transformer Test

Multiple parameters of planar transformers at 100 kHz are tested and compared in Figs. 8, 9, 10, and 11. Similar to the core test, transformers are also tested after being taken outside of the oven and cooled to room temperature.

In Figs. 8 and 9 as group P1, for both temperatures, the change trend of each parameter is similar. Transformers in 200 °C in P1 group are analyzed below. The primary inductance and resistance is continuously decreasing. However, the gradient is decreasing. A roughly 30% decrease is obtained from the primary inductance $L_{\mathrm{m}} + L_{\sigma}$, while the primary resistance $R_{\mathrm{m}} + R_{1\sigma}$ decreases by 70%. The decrease of the inductance is regarded as the degradation of the core or the increase of air gap due to the degradation of core adhesive

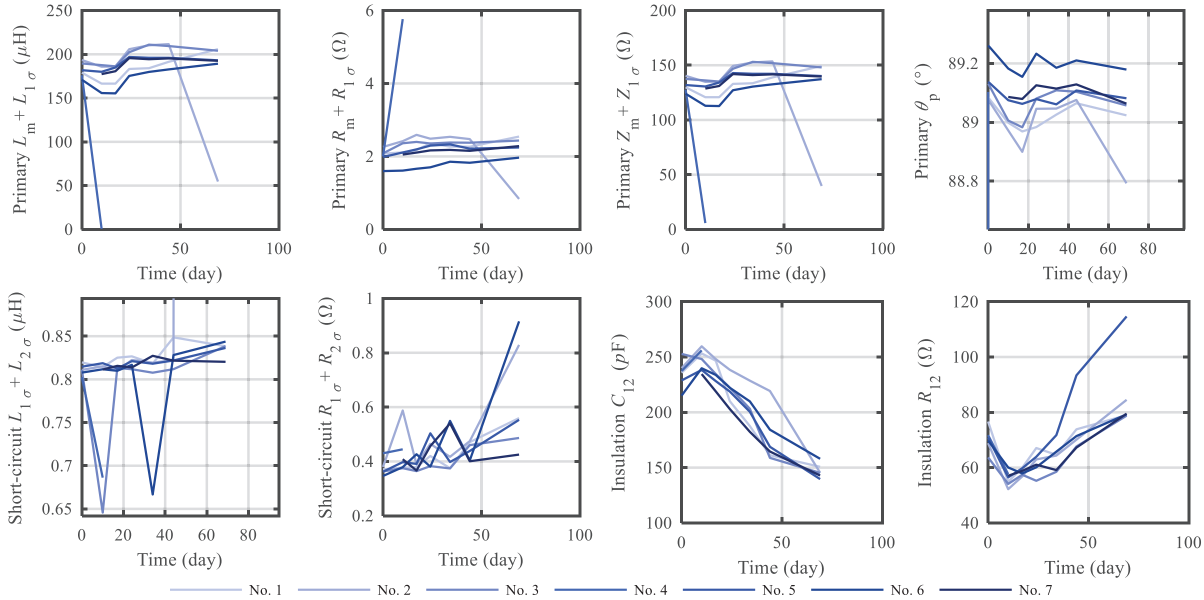

Fig. 10: Test results of No. 1 to 7 planar transformers in P2 group, 200 °C, 69 days, the related parameters are illustrated in Fig. 4(a).

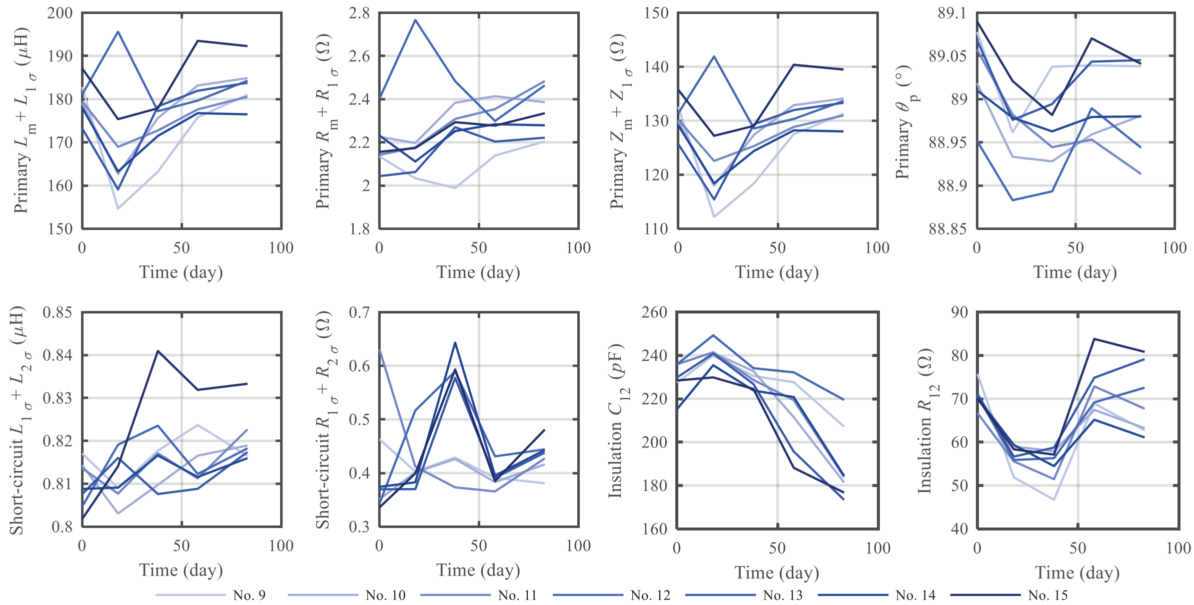

Fig. 11: Test results of No. 8 to 15 planar transformers in P2 group, 180 °C, 83 days, the related parameters are illustrated in Fig. 4(a).

paste. The decrease of the resistance is due to the core and winding.

The short-circuit $L_{1\sigma} + L_{2\sigma}$ is mainly dependent on the permeability of the air and insulation material. It is also slightly affected by the core for its the magnetic field control function. The permeability of the air and insulation is not affected much over aging, so does the short-circuit $L_{1\sigma} + L_{2\sigma}$. The short-circuit resistance $R_{1\sigma} + R_{2\sigma}$ is mainly dependent on the winding, and it increases slightly (about 25%) before 69 days. This is probably due to the oxidation of the copper layer. The divergent distribution result of $R_{1\sigma} + R_{2\sigma}$ at 90 days is probably due to the measurement error.

The insulation capacitance C_{12} and resistance R_{12} between the primary and secondary winding depend on the insulation material. The measured insulation resistance is in the range of hundreds of Ω, which is relatively small. It is probably caused by the revolution limitation of the current sensor in the impedance analyzer. However, the measured value is stable and the change trend is still meaningful for the degradation observation. An approximate of 35% decrease is observed for C_{12}, while a about 70% rise is seen for R_{12}. They are the indications of degradation. From the visual inspection in Fig.

1 (f), the insulation layer between the PCB winding layers is yellow transparent and does not change the color at this moment, and the solder mask on the PCB winding turns from green to black, which is a failure indication. However, the insulation function of the planar transformer is mainly provided by the insulation layer, and the slow degradation of it helps for the reliability.

In Figs. 10, and 11 as group P2, all the parameters in both temperatures also show a similar variation trend. However, their trends are not the same as those in P1 group. This is probably due to the different core and insulation materials applied in P1 and P2. Due to the relative slow change ratio and page limitation in the paper, their trends are not analyzed in detail here.

To summarize, there are considerable degradation in the core from all the related parameters; for copper winding and insulation, some parameters are shifting with large proportion while others are not.

IV. Conclusions

This paper presents the first observations in the degradations of planar magnetics. In order to determine the degradation indicators, various parasitic parameters are characterized before and during the degradation test. The degradation and failure mechanisms of the core, insulation, PCB winding, and the planar transformer are also investigated. The 55 days of 200 °C thermal stress leads to a considerable increase of the loss density of core specimens. The inception voltage in the partial discharge test for the planar transformer decreases with aging process, which indicates a degradation of the insulation layer. For the planar transformers, 90 days of 200 °C and 108 days of 180 °C thermal stresses are exerted and eight parasitic parameters are measured. For P1 transformer under 200 °C thermal stress, the primary inductance and resistance, and the insulation capacitance are decrease by about 30%, 70%, and 35%, respectively, while the leakage resistance and the insulation resistance are increased by around 25% and 70%, respectively. Compared to the high voltage PD test, the determination of the RLC parameters of planar magnetics is more convenient. They are with a good potential for the indicator of degradation or failure status. The up-to-failure test results of the specimens will be reported in a future paper.

Acknowledgment

The authors would like to thank Dr. Shuai Liu for the generous help during the samples test.

TABLE I: Up-to-now transformer failure summary

P1			
Number of transformer	1	3	11
Failure test time (days)	90	90	108
Failure reason	a	a	b
P2			
Number of transformer	2	4	
Failure test time (days)	69	10	
Failure reason	c	c	
Failure reasons category			
a. Pin broken during soldering			
b. Broken during transferring			
c. Inner short circuit/ core failure			

References

[1] Z. Ouyang, O. C. Thomsen, and M. A. E. Andersen, "Optimal design and tradeoff analysis of planar transformer in high-power dc-dc converters," *IEEE Trans. Ind. Electron.*, vol. 59, no. 7, pp. 2800–2810, Jul. 2012.

[2] M. Fu, C. Fei, Y. Yang, *et al.*, "Optimal design of planar magnetic components for a two-stage GaN-based DC/dc converter," *IEEE Trans. Power Electron. (Early Access)*, Jun. 2018.

[3] W. Huai, M. Liserre, F. Blaabjerg, *et al.*, "Transitioning to physics-of-failure as a reliability driver in power electronics," *IEEE J. Emerg. Sel. Top. Power Electron.*, vol. 2, no. 1, pp. 97–114, 2014.

[4] Micrometals, "Power conversion & line filter applications," https://www.micrometals.com, Tech. Rep., 2007.

[5] CoilCraft, "Notes on thermal aging in inductor cores," https://www.coilcraft.com/pdfs/Doc1192_Notes_on_ thermal_ aging.pdf, Tech. Rep., 2014.

[6] C. A. Stergiou and V. Zaspalis, "Cobalt-induced performance instabilities of mn–zn ferrite cores," *IEEE Trans. Magn.*, vol. 54, no. 8, pp. 1–8, Aug. 2018.

[7] S. S. Gorelik, B. E. Levin, L. M. Letyuk, *et al.*, "Mechanism of aging in magnesium-manganese-zinc ferrite," *Soviet Physics Journal*, vol. 10, no. 7, p. 14, Jul. 1, 1967.

[8] TDK Corporation, "Ferrite for telecommunication summary," Tech. Rep., Apr. 2011.

[9] T. Matsmura, K. Nagayama, S. Hagimura, *et al.*, "Long term reliability of iron-based amorphous alloy cores for oil-immersed transformer," *IEEE Trans. Magn.*, vol. 26, no. 5, pp. 1993–1995, 1990.

[10] Q. Zhong, "Power transformer end-of-life modelling: Linking statistics with physical ageing," PhD dissertation, Manchester, UK: The University of Manchester, 2012.

[11] IEEE Power & Energy Society, *IEEE Guide for Loading Mineral-Oil-Immersed Transformers and Step-Voltage Regulators*, Mar. 2012.

[12] P. Mancinelli, S. Stagnitta, and A. Cavallini, "Lifetime analysis of an automotive electrical motor with hairpin wound stator," in *Proc. 2016 IEEE Conf. Electrical Insul. Dielectric Phenomena*, IEEE, Oct. 2016, pp. 877–880.

[13] C. Sciascera, M. Galea, P. Giangrande, *et al.*, "Lifetime consumption and degradation analysis of the winding insulation of electrical machines," in *Proc. 8th IET Int. Conf. Power Electron. Machines Drives*, Apr. 2016, pp. 1–5.

[14] S. Zhan, M. H. Azarian, and M. Pecht, "Reliability of printed circuit boards processed using no-clean flux technology in temperature–humidity–bias conditions," *IEEE Trans. Device Mat. Rel.*, vol. 8, no. 2, pp. 426–434, 2008.

[15] *Military handbook: Reliability prediction of electronic equipment*, Standard MIL-HDBK-217F, Dec. 1991.

[16] *Reliability Prediction Procedure for Electronic Equipment*. Telcordia Technologies, Inc. NJ, USA, 2011.

[17] CoilCraft, "Failure rate calculation," https://www.coilcraft.com/pdfs/doc292_fit_failure_rate.pdf, Tech. Rep.

[18] V. J. Thottuvelil, T. G. Wilson, and H. A. Owen, "High-frequency measurement techniques for magnetic cores," *IEEE Trans. Power Electron.*, vol. 5, no. 1, pp. 41–53, Jan. 1990.

[19] E. Kuffel, W. Zaengl, and J. Kuffel, *High Voltage Engineering: Fundamentals*. Oxford, UK: Newnes, 2000.

[20] International Electrotechnical Commission (IEC), *IEC Standard 60270. High-voltage test techniques - Partial discharge measurements*, Geneva, Switzerland, 2000.